

22 **Abstract**

23 The unstable nature of freshwater ponds in arid landscapes represent a sizable challenge
24 for strictly aquatic organisms, such as fishes. Yet the Arabian Desert, bordering the
25 coastline of the Red Sea, plays host to a species very well adapted to such extreme
26 environments: the Arabian pupfish, *Aphanius dispar*. In this study, we estimated patterns
27 of hydrological connectivity; population structure and stable isotope for samples of *A.*
28 *dispar* living in small, isolated ponds of nearly-freshwater in the Arabian desert and
29 highly saline coastal lagoons along the Red Sea. The genomic and hydrological analyses
30 indicate that populations are largely separated by drainage origin, as fish from desert
31 ponds appear to be transported to coastal lagoons of the Red Sea along ephemeral river
32 systems arising from flash flood events. Further, our study indicates there is an ecological
33 change when being washed from pond environments to coastal waters, due to a
34 significant shift in muscle stable isotopes ratios between both groups. Considering that
35 the genetic breaks are mostly observed between drainage origin, this study suggests that
36 *A. dispar* can survive large changes in salinity and ecological regimes over small time-
37 scales.

38

39 **Introduction**

40 Population dynamics are often defined and restricted by differences in environmental
41 conditions. A growing body of research shows that environmental gradients are often a
42 driver for selection, but also population structure, as adaptation to local conditions can
43 lead to selection of particular genotypes on either side of an ecological break (Wang &
44 Bradburd, 2014). Differences in fitness and conditioning across such ecological gradients
45 can lead to restricted dispersal or even dispersal barriers, which in turn can significantly
46 shape the population structure at relatively small geographic scales (Sexton, Hangartner,
47 & Hoffmann, 2014). This concept is tremendously important in evolutionary biology, as
48 ecological gradients have been suggested as one of the initial mechanisms of divergence
49 that can promote speciation of lineages (Doebeli & Dieckmann, 2003).

50

51 A small number of species have the ability to traverse ecological barriers, even
52 significant dispersal barriers and eventually conquer some of the world's extreme
53 environments, via physiological and behavioural adaptations (Kelley et al., 2014; Moore,
54 Cooper, Biewener, & Vasudevan, 2017). Among the most intriguing of these examples
55 are fishes that live in desert environments, as they inhabit highly isolated and often
56 ephemeral ponds in very arid landscapes. It is assumed that most of these species have
57 high phenotypic plasticity, as these fishes encounter ephemeral streams (Furness, 2016),
58 large temperature fluctuations (Bennett & Beitinger, 1997), extreme changes in water
59 chemistry (Kavembe, Franchini, Irisarri, Machado-Schiaffino, & Meyer, 2015) and high
60 spatiotemporal variability in water supply (Fisher, Gray, Grimm, & Busch, 1982).
61 Among the main questions regarding these particular groups of fishes, the most intriguing

62 is how such isolated populations continue to survive after an initial colonization event. It
63 is well known that isolation of populations can result in a slew of detrimental conditions,
64 such as loss of genetic variability, inbreeding depression or the accumulation of
65 deleterious mutations (Gaggiotti, 2003). Considering that population persistence and
66 long-term survival is largely influenced by genetic diversity (Bouzat, 2010), living in
67 isolated and highly restricted water bodies might threaten the persistence of desert fishes
68 over long time-scales.

69

70 Among the few fish groups that inhabit arid environments, Cyprinodontiformes exhibit
71 remarkable adaptations to extreme conditions. For example, the African turquoise
72 killifish (*Nothobranchius furzeri*) evolved an embryonic diapause, allowing fertilized
73 eggs to survive a dry period (Furness, 2016). Furthermore, killifish can also be found in
74 habitats with widely varying salinities and they are therefore categorized as euryhaline
75 (Wood & Marshall, 1994). The genus *Fundulus*, for instance, displays a wide range of
76 osmotolerant physiologies (Whitehead, 2010), with *F. heteroclitus* being able to rapidly
77 acclimate to an osmotic shock by changing its transcriptional program and later
78 remodeling its tissues (Whitehead, Galvez, Zhang, Williams, & Oleksiak, 2011). Despite
79 these remarkable adaptations, some Cyprinodontiformes occupy very restricted habitats.
80 For example, the Devils Hole pupfish (*Cyprinodon diabolis*) lives only in Devils Hole
81 (in the Amargosa Desert of Nevada) and it is described as occupying the smallest known
82 natural range (a single pool < 80 m²) for any vertebrate species (Martin, Crawford,
83 Turner, & Simons, 2016). Indeed, many species of fish inhabiting such arid landscapes
84 are currently listed as endangered (Hopken, Douglas, & Douglas, 2013; Van Haverbeke,

85 Stone, Coggins, & Pillow, 2013) and have been of conservation concern for decades
86 (Meffe & Vrijenhoek, 1988).

87

88 The Arabian pupfish, *Aphanius dispar* (Cyprinodontidae), is present in the Middle East
89 with landlocked populations in countries such as Oman, Iran and Saudi Arabia (Al-
90 Kahem-Al-Balawi et al., 2008; Freyhof, 2014; Haas, 1982; Hrbek & Meyer, 2003). This
91 species represents an interesting conundrum, as it has a large distribution range, but it
92 inhabits highly restricted ephemeral ponds with no permanent rivers around them.
93 Furthermore, from a pilot study we revealed that they are also present in coastal lagoons
94 of the Red Sea. Phylogenetic analyses of the genus suggest that this group has saltwater
95 ancestry, with the closing and drying of the Tethys Sea resulting in landlocked remnant
96 populations which likely then diverged due to the resultant strong ecological changes
97 (Hrbek & Meyer, 2003).

98

99 In this study we explore suitable habitats for *A.dispar* to live in the desert as well as the
100 Red Sea coastline in Saudi Arabia and aim to understand the population connectivity of
101 this species. We investigate the environmental conditions and population structure of *A.*
102 *dispar* in the Arabian desert by employing a multi-disciplinary approach that combines
103 hydrological predictive mapping, population genomics, stable isotope analysis, as well as
104 chemical and physical analyses of water bodies.

105

106 **Methods**

107 *Sample collection*

108 In order to acquire information on the presence of water ponds and streams in the Saudi
109 Arabian desert, extensive searches were performed using Google Earth, high-resolution
110 satellite data and through contacting local landowners and regional police. Subsequently,
111 a range of potential water ponds were identified and visited (see Figure 1). From a survey
112 of 28 locations, *Aphanius dispar* was detected at 11 sites and was collected using a 3 m
113 wide seine net. Fish length was measured, and a piece of the dorsal fin was cut and
114 placed in 96% ethanol. Fish were then returned to the pond. Individuals with fins too
115 small for finclip collection were euthanized with a blow to the head, with the entire tail
116 preserved in ethanol. All procedures were performed in accordance with relevant
117 guidelines and regulations and were approved and completed with the ethics permit
118 15IBEC35_Ravasi from the Institutional Biosafety and BioEthics Committee (IBEC) of
119 the King Abdullah University of Science and Technology.

120

121 *Stable isotopes*

122 We employed two types of stable isotope measurements: fish muscle tissue and pond
123 water isotopes. Fish muscle tissue can give indications on the diet of the fish in the ponds
124 and the sea (Zanden & Rasmussen, 2001). Water isotope analysis can indicate the
125 evaporative and flow processes of the water body. While these distinct isotopic
126 measurements have different applications, they both help to understand the biological and
127 hydrological connectivity of the ponds in the desert. Isotope ratios are reported relative to
128 their respective standards:

129 1)
$$\delta = \left(\frac{R_{sample}}{R_{standard}} - 1 \right) \text{‰}$$

130 where R_{sample} and $R_{standard}$ are the isotope ratios (heavier isotopologue to the more
131 abundant isotopologue) measured in the sample.

132

133 *a) Water stable isotope analysis*

134 Water samples from the six desert ponds were analyzed for isotope analysis at the King
135 Abdullah University of Science and Technology on a Picarro Wavelength Scanning
136 Cavity Ringdown Spectrometer (WSCRDS L115-I, Picarro Inc., Sunnyvale, CA, USA)
137 interfaced to a liquid autosampler (CTC HTC Pal liquid autosampler; LEAP
138 Technologies, Carrboro, NC, USA). $\delta^2\text{H}$ and $\delta^{18}\text{O}$ were measured and are isotope ratios
139 for $^2\text{H}^1\text{H}^{16}\text{O}$ and $^1\text{H}_2^{18}\text{O}$ isotopologues, respectively. Samples were referenced to the
140 VSMOW scale using laboratory working standards previously referenced to the
141 VSMOW2/ SLAP2 (Standard Light Antarctic Precipitation) standards. The $\delta^2\text{H}$ and $\delta^{18}\text{O}$
142 values of samples was determined using the two-point linear normalization method
143 described in Paul *et al.* (2007) (Paul et al., 2007), which calibrate sample isotope ratios
144 using the linear relationship between the true and measured isotope ratios of two working
145 standards that bracket the sample. Each measurement of standards and samples consisted
146 of 10 injections of which the last 4 were used to determine isotope ratios. Uncertainty for
147 the reported isotope values is determined by propagating the standard deviations (1σ) of
148 the last 4 injections from measurement of standards and samples.

149

150 *b) Muscle tissue stable isotope preparation and analysis*

151 For each collection site, a subset of adult fish was sacrificed, and bodies were frozen with
152 dry ice in the field. In the lab, fish were thawed, and white muscle tissue was de-skinned,
153 descaled and dried for 24 h at 60 °C. Samples were ground using a MP Bio FastPrep-24
154 instrument (6.5 m/s for 60s until pulverized, repeated 1-4 times) and Lysing Matrix E 2
155 mL tubes with 1 x 4.0 mm ceramic sphere, 30±3 1.4 mm ceramic spheres. Tissues were
156 rinsed in 1 mL 2:1 chloroform-methanol solution and shaken vigorously for 30 s to
157 remove isotope differences due to a lipid content bias, as described by Ehrich *et al.*
158 (2011) (Ehrich et al., 2011). The solution was transferred to 1.5 mL Eppendorf tubes,
159 leaving the spheres behind. The samples were left to stand for 15 minutes at room
160 temperature, and then centrifuged for 10 minutes at 3,400 rpm. The supernatant was
161 discarded, and the chloroform-methanol rinse was repeated two additional times. Samples
162 were then dried in 1.5 mL Eppendorf tubes for 24 h at 60 °C and broken apart using a
163 scoopula. Approximately 1±0.2 mg of sample was placed in tin capsules for solid
164 samples (5 x 9 mm) for the Isotope Ratio Mass Spectrometry analysis (IRMS). ¹³C
165 and ¹⁵N isotopes were analyzed using a PDZ Europa ANCA-GSL elemental analyzer
166 interfaced to a PDZ Europa 20-20 isotope ratio mass spectrometer (Sercon Ltd.,
167 Cheshire, UK) at the Stable Isotope Facility at the University of California, Davis.
168 Briefly, samples were combusted at 1000°C with chromium oxide and silvered copper
169 oxide, with a subsequent oxides removal in a reduction reactor. N₂ and CO₂ were
170 separated on a Carbosieve GC column (65°C, 65 mL/min) before entering the IRMS.
171 Samples were interspersed with replicates of two laboratory standards and isotope ratio
172 delta values were measured relative to the international standards VPDB (Vienna
173 PeeDee Belemnite) and Air for carbon and nitrogen, respectively (Sharp, 2007).

174 Statistical analyses for tissue stable isotopes were carried out using R (R version 3.4.0,
175 2017-04-21). Data were checked for normality with the Shapiro-Wilk test and for
176 homogenous variance with the Fligner-Killeen test and considered significant at $p < 0.05$.
177 The correlation between $\delta^{13}\text{C}$ and $\delta^{15}\text{N}$ was tested with a Spearman's correlation, as well
178 as the allometric effect of size on isotope contents. Since data did not satisfy conditions
179 for the use of parametric statistics, a two-way non-parametric ANCOVA in the *sm*
180 package (Bowman & Azzalini, 2014) was used to test for differences in $\delta^{13}\text{C}$ and $\delta^{15}\text{N}$
181 among sites, with fish size as the covariate. Sampling sites of *A. dispar* were split into
182 two water type groups (Desert Pond and Sea Water), as well as in four different clusters
183 (determined through genetic and hydrological analysis, stated below), depending on the
184 drainage basin they belong to (from north to south: Cluster 1 = DP1, DP2, SW1, SW2;
185 Cluster 2 = DP3, SW3; Cluster 3 = DP4, SW4; Cluster 4 = DP5, DP6, SW5). Differences
186 in fish muscle isotopic signatures between different desert pond were also evaluated.
187 Muscle mean content in $\delta^{13}\text{C}$ and $\delta^{15}\text{N}$ and standard deviation for the different sites (n:
188 DP3 =11, DP4 = 11, all others = 12) were calculated and visualized in R.

189

190 *Water parameters and samples*

191 To quantify the water chemistry of the desert ponds and better understand the
192 environmental conditions of the fish habitat, we took *in situ* measurements as well as
193 collected water samples for later analyses. A portable Ocean Seven 305 Plus CTD
194 (Idronaut) was used to measure temperature, pressure, conductivity, salinity, percent
195 oxygen saturation, parts per million of O_2 and pH on site. The CTD sonde was submersed
196 at a depth of approximately 30 cm and left to acclimate for one minute. Five minutes of

197 measurements were taken at a sampling rate of 5 seconds, with the total of 60 data points
198 averaged to provide a single value for each parameter per site (referred to as “average
199 temperature”). Water samples at each site were collected in 500 ml HDPC containers,
200 either filled only with water for isotope and water analysis, or with 2ml of 5% nitric acid
201 for preservation for chemical water analysis. Water samples were analyzed using Ion
202 Chromatography. Seawater samples (sites SW1 – SW5) were diluted x10 and filtered
203 using Dionex OnGuard II Ba/Ag/H 2.5 cc cartridges to remove SO_4^{2-} and Cl^- . Standards
204 and water samples were transferred to Autoselect Polyvial 10 mL vials and covered with
205 septa and caps. Samples were run on Dionex ICS-3000 with the Chromeleon
206 Chromatography Management System (version 6.7) program and using an autosampler.
207 Photometric analysis was performed on water samples to measure for chlorides, sulphates
208 and silica. Standards were run accordingly (chlorides: 0 ppm, 20 ppm, 200 ppm;
209 sulphates: 0, 30 and 100 ppm; silica: 0, 100 and 500 ppb). Water samples were
210 transferred to cuvettes and loaded into an Aquakem 250 (Thermo Scientific) for analysis.
211 For samples that were outside of standard ranges, samples were diluted appropriately (see
212 Supplementary materials) and re-run.

213

214 *Streamflow mapping*

215 To establish the hydrological connectivity from the desert highlands to the Red Sea
216 coastline (and the resultant possible genetic links between the locations where pupfish
217 were present), we needed to determine the predominant flow direction at each cell of an
218 underlying topographic model. The ArcGIS-based hydrology toolset was used for the
219 extraction and analysis of watersheds and streamflow, using the Advanced Spaceborne

220 Thermal Emission and Reflection Radiometer (ASTER) Global Digital Elevation Model
221 (ASTGTM, JPL 2009) to provide a topographic description of the region. Raw ASTER
222 data, distributed by NASA as GeoTIFF files, have a 30 m spatial resolution and are
223 referenced to the WGS84 coordinate system. Supplementary Figure 1 shows the flow
224 process of delineating watershed boundaries and stream networks from a digital elevation
225 model (DEM). To ensure that any water “flow” can move from one cell to any adjacent
226 cell, a depressionless DEM was obtained by filling any localized “sinks” that might have
227 formed as an artefact of the interpolation process. From this, the natural flow direction (as
228 dictated by the direction of steepest descent) and the flow accumulation per cell (i.e. the
229 number of upstream cells “draining” to that particular cell) can then be calculated. Only
230 those cells with a high accumulation threshold (>1000 contributing cells) are considered
231 to represent a dominant flow path. A streamline can be produced by connecting these
232 cells. Watershed boundaries are delineated automatically based on the natural water
233 divides, which follow the highest elevations in the DEM. Using Google Earth imagery
234 (Google Earth 7.1.2.2041; December 31, 2016) as an underlying base map, we can
235 determine the potential connectivity routes for fish by following delineated streamlines
236 from the highest sampled locations on the mountains, to the lowest points near the
237 shoreline. A visual interrogation of satellite images allowed elements such as dams,
238 bridges, culverts and agricultural regions to be identified and to manually edit segments
239 along the streamlines.

240

241 *DNA extractions and Restriction Site Associated DNA Sequencing (RAD-Seq)*

242 To understand the genetic population structure and genetic connectivity of *A. dispar* we
243 used 5 mm pieces of fin clip from each individual sample for 28-29 individuals per site
244 (at 11 sites) to extract DNA with 96-well DNA extraction kits from Qiagen (DNeasy 96
245 Blood and Tissue Kit) or Macherey-Nagel (NucleoSpin 96 Tissue). The manufacturer
246 protocols were followed with a deviation of 8-10 hours of lysis and elution in 50 μ l H₂O.
247 Concentrations were measured with a Qubit 2.0 fluorometer with a dsDNA High
248 Sensitivity reagent kit. We used a modified double digest (ddRad) protocol (Peterson,
249 Weber, Kay, Fisher, & Hoekstra, 2012). Briefly, DNA was digested using SphI High
250 Fidelity and MluCI High Fidelity enzymes with the appropriate CutSmart Buffer (New
251 England Biolabs) and cleaned with AMPURE XP beads. Adapters were ligated to 100 ng
252 of digested DNA with a combination of sixteen adapters and eleven indices to uniquely
253 identify individual samples out of 80 multiplexed samples in one sequencing lane. Pools
254 were created from equally concentrated and cleaned samples and size selected in a
255 BluePippin (Sage Science) with 2% Gel Cassettes to a size of 300bp. We used a KAPA
256 Hifi Ready Mix for the PCR amplification with ten PCR cycles and temperatures
257 according to the manufacturer. Samples were run on a bioanalyzer (Agilent) and a qPCR
258 (7900 HT Fast Real Time PCR system, ABI) was used to quantify and combine all 80
259 samples within one library at equimolar concentration. Four libraries were then
260 sequenced paired-end on an Illumina HiSeq2000 to a length of 100bp at the KAUST
261 Bioscience Core Lab facility.

262

263 *RAD-Seq data processing*

264 Raw sequence fastq files were de-multiplexed for each lane of Illumina using
265 *process_radtags* in the software STACKS 1.40 (Catchen, Hohenlohe, Bassham, Amores,
266 & Cresko, 2013). All sequences were quality trimmed with Trimmomatic 0.33 (Bolger,
267 Lohse, & Usadel, 2014) with a Phred score quality cutoff of 30. Individuals with less than
268 300,000 remaining first read sequences (from paired end reads) were removed from the
269 analysis. Due to the lack of a reference genome for this species, we ran the quality
270 trimmed first read files through the *denovo_map* perl script in STACKS. The final
271 optimized parameters were set to a conservative number of mismatches allowed (-n 2 and
272 -M 2), a minimum number of identical reads to form a stack was three and SNP calling
273 was performed with an upper bound error rate of 0.05 (--bound_high 0.05). After the
274 putative SNP detection, the function *populations* was run to select putative SNPs meeting
275 several criteria. The variant had to have a minimum read number of 10 (-m 10), be
276 present in at least seven of the eleven locations (-p 7) and in more than 20 individuals per
277 locations (-r 0.72). A minimum allele frequency filter of 0.05 was applied and we chose
278 to use one randomly putative SNP from each stack. The resulting vcf file was converted
279 into different input file formats for further analysis using PGDSPIDER (Lischer &
280 Excoffier, 2012). To avoid a bias due to duplicated sequences across the genome,
281 putative SNPs were discarded if heterozygosity was higher than 0.5 (calculated with
282 *vcftools*, following (Danecek et al., 2011) and if the mean read depth was a median
283 absolute deviation away from the median depth (Seeb et al., 2014). Hardy-Weinberg
284 exact tests were performed in Genepop version 4.6 (Rousset, 2008) and putative SNPs
285 were removed if there was a significant deviation in more than four of the eleven

286 locations for which tests could be performed. All SNPs that did not pass the criteria were
287 blacklisted in *populations* and removed from further analysis.

288

289 *Population genetics and clustering analyses*

290 Population genetics metrics such as average allele number, private alleles, inbreeding
291 coefficient and locus and pair-wise F_{ST} were obtained for the set of filtered final SNPs
292 with *populations*. VCFtools v0.1.13 was used to look at minor allele frequencies, Hardy-
293 Weinberg equilibrium and locus and population heterozygosities (Danecek et al., 2011).
294 Pairwise AMOVA F_{ST} values for population differentiation measures and significance
295 ($p < 0.05$) were obtained in GenoDive V2.0b27 using 10,000 permutations as well as the
296 pairwise kinship coefficient r (Meirmans & Van Tienderen, 2004). Effective population
297 sizes were calculated in NeEstimator using the linkage disequilibrium method including
298 all final selected SNP loci (Do et al., 2014). Here we present the results of the largest
299 harmonic mean sample size per population.

300 To evaluate genetic structure among all sampled individuals, we performed a principal
301 component analysis (PCA) as well as Bayesian clustering analysis. The PCA was
302 computed in the *adegenet* package v. 2.0.1 in R (Jombart, 2008). We represent the
303 eigenvalues of the analysis revealing the variance of each principal component and a
304 scatterplot summarizing the genetic diversity including the center ellipses per sampling
305 location. Clustering analysis was performed in Structure v.2.3.4 (Pritchard, Stephens, &
306 Donnelly, 2000) under the admixture model with a 10% burn-in period and 500,000
307 iterations of Markov Chain Monte Carlo (MCMC), which creates a probability
308 distribution and allows for the evaluation of the likeliness of different numbers of clusters

309 (K) within the dataset. Ten replicates were run for each putative number of clusters (K)
310 with K ranging from 1 to 11. The results were then passed through STRUCTURE
311 HARVESTER v0.6.94 (Earl & vonHoldt, 2012) to apply the *ad hoc* statistic delta K
312 proposed by Evanno and coauthors (2005). Resulting individual and population files
313 were used in CLUMPP v1.1 (Jakobsson & Rosenberg, 2007) and DISTRUCT v1.1
314 (Rosenberg, 2003) to combine all STRUCTURE runs and visualize the results.

315

316 *Loci under selection*

317 As *A. dispar* individuals were found in very different habitat types (from desert ponds to
318 the highly saline waters of the Red Sea) we tested for possible selection in any of the
319 analyzed loci possibly indicating adaptive processes to the environmental conditions. For
320 this we re-ran the *populations* program with the same whitelist of 5,955 loci selecting
321 specific locations. First, all locations were used by defining all desert pond locations as
322 one population and all seawater location as another one, in order to evaluate global
323 selection between desert and seawater habitats. However, adaptive processes might differ
324 for the different desert ponds and we therefore sub-selected locations. We evaluate
325 adaptive loci for DP1 & DP2 against SW1 & SW2, DP3 vs. SW3, DP4 vs. SW4, and
326 DP5 & DP6 against SW5. Each resulting vcf files was format converted with PGDSpider
327 2.0.0.2 (Lischer & Excoffier, 2012). For outlier loci detection we used a Bayesian
328 approach incorporated in Bayescan v2.1 (Foll & Gaggiotti, 2008). Briefly, posterior odds
329 of a locus being under selection are obtained with MCMC with the help of the proportion
330 of loci exhibiting large F_{ST} in comparison to other loci. To further minimize the number
331 of false positives, the prior odds was increased to 100 (-pr_odds 100). Outlier loci were

332 then visualized and selected in R after applying a False Discovery Rate (FDR) of 0.05.

333 Sequence reads for resulting putative loci under selection were then blasted against the

334 NCBI nr database (blastn) and successful blast hits are presented if the evalue was below

335 $1e^{-5}$.

336

337 **Results**

338 *Pupfish locations, collection and pond properties*

339 Due to the lack of previous knowledge on the locations of the Arabian pupfish
340 populations in western Saudi Arabia, we sampled 28 sites, of which only eleven had
341 pupfish present (Figure 1). 12 Red Sea coastline sites and 16 inland enclosed ponds or
342 streams were visited (Table 1 & Supplementary Table 1); 6 inland sites and 5 seawater
343 sites had *Aphanius dispar* specimen. For two inland ponds, no sonde measurements could
344 be obtained due to complications transporting the CTD (conductivity, temperature and
345 depth) sonde into the steep canyons. Five ponds contained freshwater with a salinity
346 upper maximum threshold of 0.5 ppt, whereas salinity in the other nine measured ponds
347 ranged from 0.54 to 1.45 ppt. Most of the ponds therefore consisted of brackish water.
348 *Aphanius dispar* was only found in ponds with salinities higher than 0.74 ppt. pH ranged
349 between 7.71 to 9.41 across all sites, with the majority exhibiting a pH between 8 and 9.
350 The average temperature in the inland ponds was 28.9 °C (± 4.9 SE), while in the Red Sea
351 sites it was 21.9 °C (± 4.17 SE). Sampling of fish was performed during the late boreal
352 autumn and early winter months (i.e., November-January), hence during the period of
353 lowest temperature of the year. The highest average water temperature, 38.4 °C, was
354 observed at the Al Lith hot spring. At this site, pupfish live in higher temperatures in
355 comparison to all other sites, as well as with larger water content of silica (80,470 ppb).
356 These results illustrate the wide range of environments which pupfish populations are
357 able to exploit along the Red Sea coast.

358

359 *Water stable isotopes*

360 To further understand environmental conditions of the six inland ponds inhabited by *A.*
361 *dispar*, water samples were collected, and their stable oxygen and hydrogen isotopes
362 measured (Supplementary Table 1). This can aid in understanding the source of the water
363 in the desert pond and if evaporation occurs comparatively, which can indicate water
364 flow or standing waters. A strong linear relationship between the $\delta^2\text{H}$ and $\delta^{18}\text{O}$ of these
365 samples was observed, with a slope of 4.83. Supplementary Figure 2 shows the linear
366 regression of measurements, with data exhibiting a low slope compared to the Global
367 Meteoric Water Line (GMWL). The relatively low slope indicates samples were subject
368 to significant evaporative enrichment (Gat, 1996; Gibson, Birks, & Edwards, 2008;
369 Gibson & Reid, 2014). The linear relationship between $\delta^2\text{H}$ and $\delta^{18}\text{O}$ across all samples
370 indicates a common water source derived from a single recharge event, with variability
371 between samples caused by the degree of evaporative enrichment for each water pool.
372 This is consistent with observations made at each site, with DP1 and DP2 being the two
373 most stagnant ponds with the least oxygen and greatest $\delta^2\text{H}$ and $\delta^{18}\text{O}$ isotopic enrichment
374 (Table 1).

375

376 *Streamflow mapping*

377 The overall topography of the study region is a mountainous inland region that is
378 bounded to the east by the Arabian shield, and which drains westward to a flatter desert
379 terrain towards the Red Sea coastline. In order to understand the hydrology of the area
380 and the exact hydrological constraints for the Arabian pupfish we created streamflow
381 maps for each sample location derived from a satellite-based digital elevation model.
382 Using the derived stream networks, a total of 6 different migration pathways were

383 identified within the study area (Figure 2 & Supplementary Table 4). Figure 2 illustrates
384 the digital elevation model (DEM) based hydrological connectivity as streamlines
385 flowing from each of the desert site locations where pupfish were present. We find that
386 during periods of occasionally intense or sustained rainfall, the desert ponds may become
387 hydrologically connected to their downstream saltwater location through tributary and
388 main stem water flow. Four distinct areas of potential hydrological connectivity can be
389 determined from Figure 2. In the northern portion of our study region, water from DP1
390 and DP2 are hydrologically linked via defined streamlines to SW1. SW2 serves as a
391 regional seawater sample pair for SW1, as it is separated by a distance of approximately
392 40 km. Further south, there is delineated connectivity between DP3 and SW3, as well as
393 between DP4 and SW4. In the southernmost part of the sampling area, DP6 has a
394 tributary stream that connects with SW5, while DP5 has a separate watercourse to the
395 sea. It is important to note that these streamlines do not represent active flow paths, as
396 Saudi Arabia has no permanent rivers. Instead, the streamlines describe either
397 permanently or intermittently dry riverbeds, defined as a function of the topography, with
398 ephemeral flows only occurring in cases of sufficient rainfall.

399

400 *RAD-sequencing*

401 In order to verify the potential hydrological connectivity for the Arabian pupfish, we use
402 Single Nucleotide Polymorphism (SNPs) genetic markers to evaluate the genetic
403 population connectivity of *Aphanius dispar*. For this we genotyped between 28 and 30
404 individuals per site for the eleven *A. dispar* locations by means of RAD-sequencing
405 (Table 2 & Supplementary Table 2). Over 2 million sequence reads were obtained on

406 average for each individual. Six samples were removed from further analysis as they had
407 fewer than 300,000 reads after demultiplexing and quality trimming, resulting in 27 to 30
408 individual samples per location. The total final sample number was 314 individuals for 11
409 sites (five saltwater and six desert pond localities) (Figure 1). A total of 690,084 putative
410 single nucleotide polymorphisms (SNPs) were obtained with STACKS (Catchen et al.,
411 2013), which were stringently filtered to a final 5,955 SNP loci. The average depth of
412 coverage for these loci was 48x, with a minimum of 24x and an average minor allele
413 frequency of 0.21 (Supplementary Figures 4 & 5).

414

415 *Population genomics*

416 The number of alleles across the 5,955 SNP loci ranged from 1.3 to 1.8 for the different
417 locations (Table 2). Heterozygosity revealed lower levels for desert ponds and
418 particularly for desert pond DP4 the lowest heterozygosity among all locations, while
419 also having a negative inbreeding coefficient (F_{IS}). DP4 also exhibited the most private
420 alleles (27) followed by DP1 with 15 and SW2 with 13. Three seawater locations SW3-
421 SW5 had no private alleles. Pairwise genetic distance between populations (F_{ST}) was
422 highest for DP4, with almost all values above 0.2 and the closest genetic distance with
423 SW4 (Figure 3). The lowest value (0) was observed for DP1 and DP2. Interestingly, most
424 DP locations showed higher F_{ST} values when compared to other DP localities than with
425 SW locations, indicating a clear disconnection between desert pond sites. Exceptions to
426 this include DP5 and DP6, with an F_{ST} value of 0.048. Pairwise F_{ST} comparisons between
427 seawater localities ranged between 0.005 to a maximum of 0.105 (SW2 vs SW5).

428 Effective population size ranged between a very low 51 in DP4 to nearly 6,000 in SW2
429 (Table 2). DP3 was the only other site with an effective size below 1,000.
430 Bayesian clustering and *ad hoc* testing allowed for the approximation of the most likely
431 number of clusters within the analyzed samples. The most probable cluster numbers were
432 2 or 8, but delta K *ad hoc* testing also showed a peak at K=4 (Supplementary Figure 6).
433 K=2 divides the northern localities (DP1, DP1& SW1, SW2) from the southern sites,
434 with DP3 and SW3 being an admixed group. When considering four different genetic
435 units in our data set, a division from north to south is found, combining desert ponds and
436 seawater locations together into clusters (Figure 4). In this scenario, DP4 stands out as the
437 only locality with its own cluster. SW4 in turn seems to have the most genetically
438 admixed individuals of all locations. By increasing the cluster number to 8, a further
439 subdivision in the northern part can be found, separating the two desert ponds from the
440 seawater locations (DP1 & DP2 and SW1 and SW2). Here SW4 and SW5, the two
441 furthest southern seawater sites, appear to share some unique traits (represented by the
442 yellow cluster in Figure 4b), which are not shared with the southern desert ponds.

443

444 *Hydrological and genetic connectivity*

445 The population clustering in the principal component analysis revealed a break between
446 the four northern locations (SW1, SW2, DP1 and DP2) and the seven southern ones,
447 regardless of them being desert ponds or seawater sites (Figure 5a). The two desert
448 ponds DP1 and DP2 closely clustered together as well as the two seawater locations
449 (SW1 and SW2), with some distance between the two different environments. This

450 disjunction, however, is not seen through hydrological mapping, as DP1 & DP2 have
451 hydrological connectivity to SW1.

452

453 Since annual rainfall volume tends to increase from the north towards the south (i.e.
454 heavier and more frequent rainfalls towards the south (El Kenawy & McCabe, 2016)), the
455 likelihood of genetic connectivity might also be expected to increase amongst the
456 southern sample sites. In fact, with the exception of DP4, a decrease in genetic distance
457 between locations from the northern area to the south one was found. Moreover, in the
458 southern parts of the study area, less genetic distance was found between desert pond and
459 the nearest seawater location (DP3 with DP4; DP4 with SW4 as well as DP5, DP6 and
460 SW5). This is in accordance with the hydrological map, where water flow is possible
461 from the desert pond sites to the respective wadi (ephemeral river systems appearing
462 during intense rain periods) outlets in the Red Sea. It is not unusual for significant flow
463 events or even flash-floods to occur on an annual, or multi-annual basis (Deng et al.,
464 2015), potentially providing the mechanism behind the observed genetic connectivity
465 within the population clusters. When evaluating the third principal component, large
466 genetic distance between DP4 and most other locations becomes apparent (Figure 5b).

467

468 *Putative environmental selection*

469 Possible selective processes to different environmental condition were evaluated using an
470 F_{ST} outlier approach. All desert pond locations were grouped together and compared with
471 all seawater locations, resulting in five outlier loci (Table 3). Based on the population
472 genetic analyses, subsets of desert ponds and genetically close seawater locations were

473 evaluated separately as well. In the northern part, the analysis included two desert ponds
474 (Desert Pond (DP)1 & DP2) and two seawater locations together (Sea Water (SW) 1 &
475 SW2), and resulted in one outlier loci which was also detected during an analysis that
476 included all sites. The comparison of DP4 and SW4 resulted also in one outlier.
477 Comparing DP3 and SW3 recovered one locus only, whereas the three southernmost
478 locations exhibited ten outliers. There is no common overlapping outlier loci detected
479 among the independent salt versus desert pond comparisons. Out of the 21 unique outliers
480 detected in the different subsets of data, 10 could be successfully identified by homology
481 using BLAST, and include several genes involved in immune response and ion channels.
482 The list of NCBI description and accession number can be found in Table 3.

483

484 *Muscle tissue stable isotopes*

485 To investigate further into differences between locations and environmental influence on
486 *A. dispar* we analyzed nitrogen and carbon stable isotopes in fish white muscle tissues.
487 These analyses revealed a clear separation between pupfish from inland ponds and
488 saltwater Red Sea habitats (Figure 6). The mean values for $\delta^{13}\text{C}$ and $\delta^{15}\text{N}$ for desert pond
489 fish (DP) ranged between -21.49‰ and -26.28‰ (SD: 2.39‰ to 3.82‰) and 12.63‰ and
490 21.03‰ (SD: 1.62‰ to 4.31‰), respectively. Saltwater fish (SW) isotope mean values
491 ranged between -6.13‰ and -11.62‰ for $\delta^{13}\text{C}$ (SD: 1.21‰ to 1.58‰) and between
492 5.92‰ and 10.90‰ for $\delta^{15}\text{N}$ (SD: 0.61‰ to 1.25‰). Overall, DP sites were more
493 depleted in $\delta^{13}\text{C}$ than SW, but had the highest values of $\delta^{15}\text{N}$. The isotopic signatures of
494 $\delta^{13}\text{C}$ and $\delta^{15}\text{N}$ correlated significantly ($p < 0.0001$, $\rho = -0.85$). While gender did not result
495 in a significant covariate ($p > 0.05$), fish length was significantly correlated with both

496 $\delta^{13}\text{C}$ ($p < 0.0001$, $\rho = -0.39$) and $\delta^{15}\text{N}$ ($p = 0.0002$, $\rho = 0.32$) values. Our data did not
497 pass the normality test (Shapiro-Wilk test, $p < 0.0001$) nor the homoscedasticity test
498 (Fligner-Killeen test, $\delta^{13}\text{C}$ $p = 0.0003$; $\delta^{15}\text{N}$ $p < 0.0001$). For these reasons, to test the
499 differences between DP and SW isotope contents correcting for fish size, a nonparametric
500 ANCOVA was used. There was a strong water type effect on both $\delta^{13}\text{C}$ and $\delta^{15}\text{N}$ fish
501 content ($p < 0.0001$). When testing the differences within clusters (cluster 1: $\delta^{13}\text{C}$ $p =$
502 0.0037 , $\delta^{15}\text{N}$ $p = 0.0039$; cluster 2: $\delta^{13}\text{C}$ $p = 0.0385$, $\delta^{15}\text{N}$ $p = 0.0352$; cluster 3: $\delta^{13}\text{C}$ $p =$
503 0.0370 ; $\delta^{15}\text{N}$ $p = 0.0350$; cluster 4: $\delta^{13}\text{C}$ $p = 0.0121$; $\delta^{15}\text{N}$ $p = 0.0141$), the same result
504 was obtained, with a strong segregation between saltwater and desert pond samples,
505 irrespective of geographic proximity. When comparing between desert ponds, DP3 is
506 significantly different from all other ponds for $\delta^{13}\text{C}$ ($p = 0.0064$) and DP4 has a
507 significantly larger $\delta^{15}\text{N}$ than the other ponds ($p=0.0239$). Muscle tissue isotopes
508 analysis therefore suggests that fish in the desert pond have different diets and therefore
509 different ecological niches relative to the populations from the Red Sea coast and some
510 desert ponds have distinct isotope signatures in comparison to other desert ponds.
511

512 **Discussion**

513 Our sampling of *Aphanius dispar* along the Red Sea coastline of the Arabian Desert
514 provides insight to previously uncharacterized sites hosting populations in both near-
515 freshwater water ponds as well as in sheltered coastal marine habitats. In contrast to the
516 often ephemeral habitats occupied by the African turquoise killifish, *Nothobranchius*
517 *furzeri* (Furness, 2016), the survival and persistence of the Arabian pupfish seems to
518 depend on constant groundwater discharge and irregular rainfall events. Hydrological
519 mapping and genetic analyses reveal that due to sporadic flash floods occurring in the
520 region (Deng et al., 2015) fish may literally be washed from desert ponds out to the Red
521 Sea. The genetic population units comprised an admixture of pupfish from the two
522 different environments, desert pond and seawater individuals. We detected four main
523 genetic clusters, which mostly grouped desert fish with Red Sea individuals based on a
524 latitudinal gradient. Due to little hydrological connectivity among desert ponds, pupfish
525 from the desert (or ‘oases’) are alternately rapidly carried out to very different
526 environmental conditions in the Red Sea along wadis during flash flood events. The
527 change in environmental condition is though not accompanied by population structure,
528 contrary to many other study systems across different environmental gradients with
529 populations differentiating with distance or environment (Sexton et al., 2014).

530

531 *Ecological acclimation*

532 Surviving a ‘washout’ event from a desert pond with less than 1 ppt in salinity to the
533 highly saline Red Sea (with an average salinity of 43 ppt) requires a considerable
534 acclimation capacity. Many killifish species are euryhaline and can tolerate large salinity

535 changes in the environment. *Fundulus heteroclitus* has been shown to undergo a large
536 range of physiological changes, from drinking rates to changes in acid base regulation
537 (Wood & Marshall, 1994). Nonetheless, *Fundulus* species, albeit tolerant to large salinity
538 ranges, have diverged into species adapted to specific environmental conditions
539 (Whitehead, 2010). Interestingly, we found the same genetic populations of *A. dispar*
540 living in both desert ponds and seawater. The hypothesized saltwater evolutionary origin
541 of the *Aphanius* genus¹⁹ provides a potential explanation for the tolerance of *A. dispar*
542 when moved from near-freshwater ponds to a highly saline environment. However, it is
543 not just temperature and salinity that differ between the desert ponds and the Red Sea
544 coastal environments. We also see an ecological divergence in tissue stable isotopes
545 between desert and seawater sites, even from within the same genetic population unit.
546 The seawater fish muscle tissues were depleted in ¹⁵N and more enriched in ¹³C than their
547 freshwater counterparts. Similar signatures have previously been found when comparing
548 freshwater and saltwater fish, although the fish species in each of the environments
549 differed (Fuller et al., 2012; Robson et al., 2016). Similarly, for anadromous species such
550 as salmon that travel from fresh to saltwater, an increase in ¹³C is exhibited when resident
551 in seawater habitats (Litz et al., 2017). Higher levels of ¹⁵N, found here for the desert
552 ponds, is often correlated with higher trophic hierarchy levels (Zanden & Rasmussen,
553 1999). For *A. dispar*, however, it is difficult to isolate the potential influences of habitat-
554 related variability in the basal isotopic values of the food web from the potential trophic
555 shifts (McMahon, Hamady, & Thorrold, 2013; Post, 2002).

556

557 *Genetic divergence*

558 Environmental differences leading to ecological divergence can drive adaptation and
559 eventually speciation (Arnegard et al., 2014). Despite large ecological difference in prey
560 and habitat niche, there is little genetic difference between the desert pond fish and the
561 geographically-corresponding seawater fish. This could give a hint that ‘washout events’
562 occur frequently enough to create enough migration from the desert ponds to the seawater
563 sites, or that, as previously shown in other killifish species (Whitehead, Roach, Zhang, &
564 Galvez, 2012), the Arabian killifish has a large capacity for rapid and long-lasting plastic
565 responses to environmental change. We found only five putative outlier single nucleotide
566 loci that could be under selection between all desert pond inhabitants and seawater fish,
567 and only three that can be functionally annotated. Perforin 1 (*prf1*), a gene to which one
568 of the outliers was successfully blasted (see Table 3), has key functions in the immune
569 response and forms part of killer T-cells, indicating a potential adaptive change to the
570 highly saline environment in the Red Sea. This particular function has been seen to be
571 conserved in many fish species (Nakanishi, Toda, Shibasaki, & Somamoto, 2011; Toda,
572 Araki, Moritomo, & Nakanishi, 2011). Interestingly, in wild salmon, perforin-mediated
573 apoptotic processes were important in survival when migrating back to freshwater
574 spawning grounds from seawater (Miller et al., 2011). Environmental changes are also
575 associated with a SNP in the ATPase Family gene 3 (*afg3*) previously attributed to stress
576 and biosynthesis and with an increased expression in trout after a starvation period
577 (Rescan et al., 2007). A hint towards its importance in seawater acclimation could be
578 related to an increase in mitochondrion-rich cells and ATPase activity due to a
579 physiological demand of acid-base and ion regulation in saltwater (Lee, Hwang, Shieh,
580 & Lin, 2000).

581

582 One of the desert ponds, the Al Lith hot spring (site DP3), had high temperatures
583 (>38°C) and a different chemical signature, such as a high amount of silica. Life in such
584 hot water could potentially provoke adaptive signals in the genome. However, only one
585 putative outlier was found for the inhabitants of the hot spring in comparison to other
586 desert ponds. therefore hinting to phenotypic plasticity, as for the case of the Magadi
587 tilapia (*Alcolapia grahami*). *Alcolapia grahami* lives in hot springs in Kenya and was
588 recently described to have the highest upper critical temperature recorded for a fish (45.6
589 °C (Wood et al., 2016)). Despite the extreme environmental conditions, genetic studies
590 did not find population differences when compared to tilapia of less extreme
591 environmental conditions at close proximity (Wilson et al., 2004; Zaccara et al., 2014).
592 Low numbers of putative outlier SNPs were also detected, suggesting some ongoing gene
593 flow and admixture (Ford et al., 2015), which could be the case for our *A. dispar* samples
594 from the Al Lith hot spring. Despite the lack of loci under selection, connectivity between
595 desert ponds is low and there is limited gene flow, as indicated by large genetic distances
596 between the hot spring and other desert ponds, suggesting isolation and divergence
597 between these habitats. For the pupfish in the hot spring, we could detect a differentiated
598 ecological signature in tissue stable isotopes compared to the other desert ponds.
599 Although contradicting the findings on the Magadi tilapia, where the hot spring site
600 revealed carbon isotope tissue enrichment (Kavembe, Kautt, Machado-Schiaffino, &
601 Meyer, 2016), *A. dispar* from the Al Lith hot spring have lower values of ¹³C in their
602 muscle tissue. One possible explanation for this result might be the turbidity of the hot

603 spring site, due to a large amount of suspended silica, as carbon stable isotope depletion
604 was previously associated with turbidity in the environment (Nahon et al., 2013).

605

606 *Anthropogenic impacts on desert fish populations*

607 Besides natural environmental conditions that are reflected in the isotopic signature of the
608 pupfish, anthropogenic impacts can also be detected. In the case of DP4, we found an
609 isotopic as well as genetic signature of human disturbance. Fish tissues here are more ^{15}N
610 enriched in comparison to other locations, which indicates an accumulation of the heavier
611 isotope element possibly due to isolation of this pond (Amundson et al., 2003; Szpak,
612 2014). In this site, there is evidence of agricultural activity, most likely utilizing
613 groundwater in the area, which in turn might lower the water table and disconnect this
614 location from others. Furthermore, there is a dam structure 15 km upstream of DP4 most
615 likely restricting the water availability downstream. Even if topographic mapping shows
616 a hydrological connection between DP4 and SW4, it seems that human interference here
617 inhibits any flow of water to the sea. This hypothesis would explain the genetic
618 differentiation for this particular site, which seems to be undergoing a population
619 bottleneck. The fish in this site have in fact an increased number of private alleles and
620 low genetic diversity, indicated by low heterozygosity. Even though the inbreeding
621 coefficient was is low, this result is most likely due to low genetic differentiation within
622 the population used in the calculation. Pairwise kinship reveals most individuals within
623 this site to be highly related, and the effective population size is very low. It therefore
624 seems that use of water in this area has isolated this population, restricting its gene flow
625 and its resilience.

626

627 In the northern part of the Saudi Arabian coast, *A. dispar* in desert ponds and saltwater
628 locations do not cluster together genetically, as it is seen in the southern parts, albeit
629 hydrological connectivity potential. Here the desert pond fish are genetically closer to
630 each other, as are the seawater fish, with a clear division between desert and Red Sea
631 sample sites. There are two plausible reasons for this disconnection. The northern regions
632 receive less rainfall (El Kenawy & McCabe, 2016) and hence any hydrological
633 connectivity between the desert and the sea will be much lower. The observed strong
634 genetic divergence though is most likely caused by the ‘upstream’ construction of the
635 Rabigh Dam (completed 2008), which was built for municipal water supply and flood
636 control. Hence, even with rain events the water, and therefore the pupfish, can no longer
637 reach the sea. For this reason, *A. dispar* populations are now diverging without the
638 presence of gene flow through new migrants. A similar anthropogenic impact was found
639 for desert fish of the Colorado River area, where natural flooding occurred regularly until
640 the construction of dams that drastically changed the water availability and had a major
641 impact on the distribution of desert fish (Hillyard, Podrabsky, & van Breukelen, 2015).

642

643 Fish living in desert regions have long been a conservation concern, with a large number
644 of such species being under threat or endangered, often due to the expansion of desert
645 agriculture and increasing global temperatures (Van Haverbeke et al., 2013). Although
646 the Dead Sea subspecies (*A. dispar richardsoni*) is considered endangered (Goren, 2014),
647 *A. dispar* itself is not considered to be endangered because it has stable populations
648 widely distributed throughout the Arabian region (Freyhof, 2014). The species’ capacity

649 to acclimate and survive challenging environmental fluctuations likely plays a major role
650 in its success in this region. However, our results show that despite the large capacity of
651 *A. dispar* to acclimate and adapt to different environments and defy the constraints of
652 living in restricted desert environments, anthropogenic water use can dramatically alter
653 the population dynamics of the Arabian pupfish.
654

655 References

- 656 Al-Kahem-Al-Balawi, H. F., Al-Ghanim, K. A., Ahmad, Z., Temraz, T. A., Al-Akel, A.
657 S., Al-Misned, F., & Annazri, H. (2008). A threatened fish species (*Aphanius*
658 *dispar*) in Saudi Arabia, a case study. *Pakistan Journal of Biological Sciences* □:
659 *PJBS*, *11* (19), 2300–2307. Retrieved from
660 <http://www.ncbi.nlm.nih.gov/pubmed/19137861>
- 661 Amundson, R., Austin, A. T., Schuur, E. A. G., Yoo, K., Matzek, V., Kendall, C., ...
662 Baisden, W. T. (2003). Global patterns of the isotopic composition of soil and plant
663 nitrogen. *Global Biogeochemical Cycles*, *17* (1).
664 <https://doi.org/10.1029/2002GB001903>
- 665 Arnegard, M. E., McGee, M. D., Matthews, B., Marchinko, K. B., Conte, G. L., Kabir,
666 S., ... Schluter, D. (2014). Genetics of ecological divergence during speciation.
667 *Nature*, *511* (7509), 307–311. <https://doi.org/10.1038/nature13301>
- 668 Bennett, W. A., & Beitinger, T. L. (1997). Temperature Tolerance of the Sheepshead
669 Minnow, *Cyprinodon variegatus*. *Copeia*, *1*, 77. <https://doi.org/10.2307/1447842>
- 670 Bolger, A. M., Lohse, M., & Usadel, B. (2014). Trimmomatic: a flexible trimmer for
671 Illumina sequence data. *Bioinformatics (Oxford, England)*, *30*, 2114–2120.
672 <https://doi.org/10.1093/bioinformatics/btu170>
- 673 Bouzat, J. L. (2010). Conservation genetics of population bottlenecks: the role of chance,
674 selection, and history. *Conservation Genetics*, *11* (2), 463–478.
675 <https://doi.org/10.1007/s10592-010-0049-0>
- 676 Bowman, A., & Azzalini, A. W. (2014). R package “sm”: nonparametric smoothing
677 methods (version 2.2-5.4). Retrieved from <http://www.stats.gla.ac.uk/~adrian/sm>,
678 http://azzalini.stat.unipd.it/Book_sm
- 679 Catchen, J., Hohenlohe, P. A., Bassham, S., Amores, A., & Cresko, W. A. (2013).
680 Stacks: an analysis tool set for population genomics. *Molecular Ecology*, *22* (11),
681 3124–3140. <https://doi.org/10.1111/mec.12354>
- 682 Danecek, P., Auton, A., Abecasis, G., Albers, C. A., Banks, E., DePristo, M. A., ...
683 Durbin, R. (2011). The variant call format and VCFtools. *Bioinformatics*, *27* (15),
684 2156–2158. <https://doi.org/10.1093/bioinformatics/btr330>
- 685 Deng, L., McCabe, M. F., Stenichikov, G., Evans, J. P., Kucera, P. A., Deng, L., ...
686 Kucera, P. A. (2015). Simulation of Flash-Flood-Producing Storm Events in Saudi
687 Arabia Using the Weather Research and Forecasting Model. *Journal of*
688 *Hydrometeorology*, *16* (2), 615–630. <https://doi.org/10.1175/JHM-D-14-0126.1>
- 689 Do, C., Waples, R. S., Peel, D., Macbeth, G. M., Tillett, B. J., & Ovenden, J. R. (2014).
690 NeEstimator v2: re-implementation of software for the estimation of contemporary
691 effective population size (N_e) from genetic data. *Molecular Ecology Resources*,
692 *14* (1), 209–214. <https://doi.org/10.1111/1755-0998.12157>
- 693 Doebeli, M., & Dieckmann, U. (2003). Speciation along environmental gradients.
694 *Nature*, *421* (6920), 259–264. <https://doi.org/10.1038/nature01274>
- 695 Earl, D. A., & vonHoldt, B. M. (2012). STRUCTURE HARVESTER: a website and
696 program for visualizing STRUCTURE output and implementing the Evanno
697 method. *Conservation Genetics Resources*, *4* (2), 359–361.
698 <https://doi.org/10.1007/s12686-011-9548-7>
- 699 Ehrich, D., Tarroux, A., Stien, J., Lecomte, N., Killengreen, S., Berteaux, D., & Yoccoz,

- 700 N. G. (2011). Stable isotope analysis: modelling lipid normalization for muscle and
701 eggs from arctic mammals and birds. *Methods in Ecology and Evolution*, 2 (1), 66–
702 76. <https://doi.org/10.1111/j.2041-210X.2010.00047.x>
- 703 El Kenawy, A. M., & McCabe, M. F. (2016). A multi-decadal assessment of the
704 performance of gauge- and model-based rainfall products over Saudi Arabia:
705 climatology, anomalies and trends. *International Journal of Climatology*, 36 (2),
706 656–674. <https://doi.org/10.1002/joc.4374>
- 707 Evanno, G., Regnaut, S., & Goudet, J. (2005). Detecting the number of clusters of
708 individuals using the software STRUCTURE: a simulation study. *Molecular*
709 *Ecology*, 14 (8), 2611–2620. <https://doi.org/10.1111/j.1365-294X.2005.02553.x>
- 710 Fisher, S. G., Gray, L. J., Grimm, N. B., & Busch, D. E. (1982). Temporal Succession in
711 a Desert Stream Ecosystem Following Flash Flooding. *Ecological Monographs*, 52
712 (1), 93–110. <https://doi.org/10.2307/2937346>
- 713 Foll, M., & Gaggiotti, O. (2008). A Genome-Scan Method to Identify Selected Loci
714 Appropriate for Both Dominant and Codominant Markers: A Bayesian Perspective.
715 *Genetics*, 180 (2). Retrieved from <http://www.genetics.org/content/180/2/977>
- 716 Ford, A. G. P., Dasmahapatra, K. K., Rüber, L., Gharbi, K., Cezard, T., & Day, J. J.
717 (2015). High levels of interspecific gene flow in an endemic cichlid fish adaptive
718 radiation from an extreme lake environment. *Molecular Ecology*, 24 (13), 3421–
719 3440. <https://doi.org/10.1111/MEC.13247>
- 720 Freyhof, J. (2014). *Aphanius dispar*.
- 721 Fuller, B. T., Müldner, G., Van Neer, W., Eryvynck, A., Richards, M. P., Cooremans, B.,
722 ... Richards, M. P. (2012). Carbon and nitrogen stable isotope ratio analysis of
723 freshwater, brackish and marine fish from Belgian archaeological sites (1st and 2nd
724 millennium AD). *Journal of Analytical Atomic Spectrometry*, 27 (5), 807.
725 <https://doi.org/10.1039/c2ja10366d>
- 726 Furness, A. I. (2016). The evolution of an annual life cycle in killifish: adaptation to
727 ephemeral aquatic environments through embryonic diapause. *Biological Reviews*,
728 91 (3), 796–812. <https://doi.org/10.1111/brv.12194>
- 729 Gaggiotti, O. E. (2003). Genetic threats to population persistence. *Ann. Zool. Fennici*, 40
730 (40), 155–168. Retrieved from [http://www.annzool.net/PDF/anz40-free/anz40-](http://www.annzool.net/PDF/anz40-free/anz40-155.pdf)
731 [155.pdf](http://www.annzool.net/PDF/anz40-free/anz40-155.pdf)
- 732 Gat, J. R. (1996). Oxygen and hydrogen isotopes in the hydrologic cycle. *Annual*
733 *Review of Earth and Planetary Sciences*, 24 (1), 225–262.
734 <https://doi.org/10.1146/annurev.earth.24.1.225>
- 735 Gibson, J. J., Birks, S. J., & Edwards, T. W. D. (2008). Global prediction of δ_A and δ^2
736 H- δ^{18} O evaporation slopes for lakes and soil water accounting for seasonality.
737 *Global Biogeochemical Cycles*, 22 (2), n/a-n/a.
738 <https://doi.org/10.1029/2007GB002997>
- 739 Gibson, J. J., & Reid, R. (2014). Water balance along a chain of tundra lakes: A 20-year
740 isotopic perspective. *Journal of Hydrology*, 519, 2148–2164.
741 <https://doi.org/10.1016/j.jhydrol.2014.10.011>
- 742 Goren, M. (2014). *Aphanius dispar* ssp. *richardsoni*.
- 743 Haas, R. (1982). Notes on the ecology of *Aphanius dispar* (Pisces, Cyprinodontidae) in
744 the Sultanate of Oman. *Freshwater Biology*, 12 (1), 89–95.
745 <https://doi.org/10.1111/j.1365-2427.1982.tb00605.x>

- 746 Hillyard, S. D., Podrabsky, J. E., & van Breukelen, F. (2015). Desert Environments. In
747 *Extremophile Fishes* (pp. 59–83). Cham: Springer International Publishing.
748 https://doi.org/10.1007/978-3-319-13362-1_4
- 749 Hopken, M. W., Douglas, M. R., & Douglas, M. E. (2013). Stream hierarchy defines
750 riverscape genetics of a North American desert fish. *Molecular Ecology*, 22 (4),
751 956–971. <https://doi.org/10.1111/mec.12156>
- 752 Hrbek, T., & Meyer, A. (2003). Closing of the Tethys Sea and the phylogeny of Eurasian
753 killifishes (Cyprinodontiformes: Cyprinodontidae). *Journal of Evolutionary*
754 *Biology*, 16 (1), 17–36. <https://doi.org/10.1046/j.1420-9101.2003.00475.x>
- 755 Jakobsson, M., & Rosenberg, N. A. (2007). CLUMPP: a cluster matching and
756 permutation program for dealing with label switching and multimodality in analysis
757 of population structure. *Bioinformatics*, 23 (14), 1801–1806.
758 <https://doi.org/10.1093/bioinformatics/btm233>
- 759 Jombart, T. (2008). adegenet: a R package for the multivariate analysis of genetic
760 markers. *Bioinformatics*, 24 (11), 1403–1405.
761 <https://doi.org/10.1093/bioinformatics/btn129>
- 762 Kavembe, G. D., Franchini, P., Irisarri, I., Machado-Schiaffino, G., & Meyer, A. (2015).
763 Genomics of Adaptation to Multiple Concurrent Stresses: Insights from
764 Comparative Transcriptomics of a Cichlid Fish from One of Earth’s Most Extreme
765 Environments, the Hypersaline Soda Lake Magadi in Kenya, East Africa. *Journal of*
766 *Molecular Evolution*, 81 (3–4), 90–109. <https://doi.org/10.1007/s00239-015-9696-6>
- 767 Kavembe, G. D., Kautt, A. F., Machado-Schiaffino, G., & Meyer, A. (2016). Eco-
768 morphological differentiation in Lake Magadi tilapia, an extremophile cichlid fish
769 living in hot, alkaline and hypersaline lakes in East Africa. *Molecular Ecology*, 25
770 (7), 1610–1625. <https://doi.org/10.1111/mec.13461>
- 771 Kelley, J. L., Peyton, J. T., Fiston-Lavier, A.-S., Teets, N. M., Yee, M.-C., Johnston, J.
772 S., ... Denlinger, D. L. (2014). Compact genome of the Antarctic midge is likely an
773 adaptation to an extreme environment. *Nature Communications*, 5, ncomms5611.
774 <https://doi.org/10.1038/ncomms5611>
- 775 Lee, T. H., Hwang, P. P., Shieh, Y. E., & Lin, C. H. (2000). The relationship between
776 ‘deep-hole’ mitochondria-rich cells and salinity adaptation in the euryhaline teleost,
777 *Oreochromis mossambicus*. *Fish Physiology and Biochemistry*, 23 (2), 133–140.
778 <https://doi.org/10.1023/A:1007818631917>
- 779 Lischer, H. E. L., & Excoffier, L. (2012). PGDSpider: an automated data conversion tool
780 for connecting population genetics and genomics programs. *Bioinformatics*, 28 (2),
781 298–299. <https://doi.org/10.1093/bioinformatics/btr642>
- 782 Litz, M. N. C., Miller, J. A., Copeman, L. A., Teel, D. J., Weitkamp, L. A., Daly, E. A.,
783 & Claiborne, A. M. (2017). Ontogenetic shifts in the diets of juvenile Chinook
784 Salmon: new insight from stable isotopes and fatty acids. *Environmental Biology of*
785 *Fishes*, 100 (4), 337–360. <https://doi.org/10.1007/s10641-016-0542-5>
- 786 Martin, C. H., Crawford, J. E., Turner, B. J., & Simons, L. H. (2016). Diabolical survival
787 in Death Valley: recent pupfish colonization, gene flow and genetic assimilation in
788 the smallest species range on earth. *Proceedings of the Royal Society B: Biological*
789 *Sciences*, 283 (1823), 20152334. <https://doi.org/10.1098/rspb.2015.2334>
- 790 McMahon, K. W., Hamady, L. L., & Thorrold, S. R. (2013). A review of
791 ecogeochemistry approaches to estimating movements of marine animals.

- 792 *Limnology and Oceanography*, 58 (2), 697–714.
793 <https://doi.org/10.4319/lo.2013.58.2.0697>
- 794 Meffe, G. K., & Vrijenhoek, R. C. (1988). Conservation Genetics in the Management of
795 Desert Fishes. *Conservation Biology*, 2 (2), 157–169. <https://doi.org/10.1111/j.1523-1739.1988.tb00167.x>
- 796
797 Meirmans, P. G., & Van Tienderen, P. H. (2004). Genotype and Genodive: two
798 programs for the analysis of genetic diversity of asexual organisms. *Molecular*
799 *Ecology Notes*, 4 (4), 792–794. <https://doi.org/10.1111/j.1471-8286.2004.00770.x>
- 800 Miller, K. M., Li, S., Kaukinen, K. H., Ginther, N., Hammill, E., Curtis, J. M. R., ...
801 Farrell, A. P. (2011). Genomic Signatures Predict Migration and Spawning Failure
802 in Wild Canadian Salmon. *Science*, 331 (6014), 214–217.
803 <https://doi.org/10.1126/science.1196901>
- 804 Moore, T. Y., Cooper, K. L., Biewener, A. A., & Vasudevan, R. (2017). Unpredictability
805 of escape trajectory explains predator evasion ability and microhabitat preference of
806 desert rodents. *Nature Communications*, 8 (1), 440. <https://doi.org/10.1038/s41467-017-00373-2>
- 807
808 Nahon, S., Richoux, N. B., Kolasinski, J., Desmalades, M., Ferrier Pages, C., Lecellier,
809 G., ... Berteaux Lecellier, V. (2013). Spatial and Temporal Variations in Stable
810 Carbon ($\delta^{13}\text{C}$) and Nitrogen ($\delta^{15}\text{N}$) Isotopic Composition of Symbiotic
811 Scleractinian Corals. *PLoS ONE*, 8 (12), e81247.
812 <https://doi.org/10.1371/journal.pone.0081247>
- 813 Nakanishi, T., Toda, H., Shibasaki, Y., & Somamoto, T. (2011). Cytotoxic T cells in
814 teleost fish. *Developmental & Comparative Immunology*, 35 (12), 1317–1323.
815 <https://doi.org/10.1016/j.dci.2011.03.033>
- 816 NASA Jet Propulsion Laboratory. (2009). ASTER Global Digital Elevation Model.
817 <https://doi.org/10.5067/ASTER/ASTGTM.002>
- 818 Paul, D., Skrzypek, G., & Fórizs, I. (2007). Normalization of measured stable isotopic
819 compositions to isotope reference scales – a review. *Rapid Communications in Mass*
820 *Spectrometry*, 21 (18), 3006–3014. <https://doi.org/10.1002/rcm.3185>
- 821 Peterson, B. K., Weber, J. N., Kay, E. H., Fisher, H. S., & Hoekstra, H. E. (2012).
822 Double Digest RADseq: An Inexpensive Method for De Novo SNP Discovery and
823 Genotyping in Model and Non-Model Species. *PLoS ONE*, 7 (5), e37135.
824 <https://doi.org/10.1371/journal.pone.0037135>
- 825 Post, D. M. (2002). Using Stable Isotopes to Estimate Trophic Position: Models, Methods
826 and Assumptions. *Ecology*, 83 (3), 703–718. [https://doi.org/10.1890/0012-9658\(2002\)083\[0703:USITET\]2.0.CO;2](https://doi.org/10.1890/0012-9658(2002)083[0703:USITET]2.0.CO;2)
- 827
828 Pritchard, J. K., Stephens, M., & Donnelly, P. (2000). Inference of population structure
829 using multilocus genotype data. *Genetics*, 155 (2), 945–959. Retrieved from
830 <http://www.pubmedcentral.nih.gov/articlerender.fcgi?artid=1461096&tool=pmcentrez&rendertype=abstract>
- 831
832 Rescan, P.-Y., Montfort, J., Rallièrè, C., Le Cam, A., Esquerré, D., & Hugot, K. (2007).
833 Dynamic gene expression in fish muscle during recovery growth induced by a
834 fasting-refeeding schedule. *BMC Genomics*, 8 (1), 438.
835 <https://doi.org/10.1186/1471-2164-8-438>
- 836 Robson, H. K., Andersen, S. H., Clarke, L., Craig, O. E., Gron, K. J., Jones, A. K. G., ...
837 Heron, C. (2016). Carbon and nitrogen stable isotope values in freshwater, brackish

- 838 and marine fish bone collagen from Mesolithic and Neolithic sites in central and
839 northern Europe. *Environmental Archaeology*, 21 (2), 105–118.
840 <https://doi.org/10.1179/1749631415Y.0000000014>
- 841 Rosenberg, N. A. (2003). distruct: a program for the graphical display of population
842 structure. *Molecular Ecology Notes*, 4 (1), 137–138. <https://doi.org/10.1046/j.1471-8286.2003.00566.x>
- 843
- 844 Rousset, F. (2008). genepop'007: a complete re-implementation of the genepop software
845 for Windows and Linux. *Molecular Ecology Resources*, 8 (1), 103–106.
846 <https://doi.org/10.1111/j.1471-8286.2007.01931.x>
- 847 Seeb, L. W., Waples, R. K., Limborg, M. T., Warheit, K. I., Pascal, C. E., & Seeb, J. E.
848 (2014). Parallel signatures of selection in temporally isolated lineages of pink
849 salmon. *Molecular Ecology*, 23 (10), 2473–2485. <https://doi.org/10.1111/mec.12769>
- 850 Sexton, J. P., Hangartner, S. B., & Hoffmann, A. A. (2014). Genetic isolation by
851 environment or distance: which pattern of gene flow is most common? *Evolution*, 68
852 (1), 1–15. <https://doi.org/10.1111/evo.12258>
- 853 Sharp, Z. (2007). *Principles of stable isotope geochemistry*. Pearson/Prentice Hall.
- 854 Szpak, P. (2014). Complexities of nitrogen isotope biogeochemistry in plant-soil
855 systems: implications for the study of ancient agricultural and animal management
856 practices. *Frontiers in Plant Science*, 5, 288.
857 <https://doi.org/10.3389/fpls.2014.00288>
- 858 Toda, H., Araki, K., Moritomo, T., & Nakanishi, T. (2011). Perforin-dependent cytotoxic
859 mechanism in killing by CD8 positive T cells in ginbuna crucian carp, *Carassius*
860 *auratus langsdorfii*. *Developmental & Comparative Immunology*, 35 (1), 88–93.
861 <https://doi.org/10.1016/j.dci.2010.08.010>
- 862 Van Haverbeke, D. R., Stone, D. M., Coggins, L. G., & Pillow, M. J. (2013). Long-Term
863 Monitoring of an Endangered Desert Fish and Factors Influencing Population
864 Dynamics. *Journal of Fish and Wildlife Management*, 4 (1), 163–177.
865 <https://doi.org/10.3996/082012-JFWM-071>
- 866 Wang, I. J., & Bradburd, G. S. (2014). Isolation by environment. *Molecular Ecology*, 23
867 (23), 5649–5662. <https://doi.org/10.1111/mec.12938>
- 868 Whitehead, A. (2010). The evolutionary radiation of diverse osmotolerant physiologies
869 in killifish (*Fundulus* sp.). *Evolution*. <https://doi.org/10.1111/j.1558-5646.2010.00957.x>
- 870
- 871 Whitehead, A., Galvez, F., Zhang, S., Williams, L. M., & Oleksiak, M. F. (2011).
872 Functional genomics of physiological plasticity and local adaptation in killifish. *The*
873 *Journal of Heredity*, 102 (5), 499–511. <https://doi.org/10.1093/jhered/esq077>
- 874 Whitehead, A., Roach, J. L., Zhang, S., & Galvez, F. (2012). Salinity- and population-
875 dependent genome regulatory response during osmotic acclimation in the killifish (*Fundulus heteroclitus*) gill, 1293–1305. <https://doi.org/10.1242/jeb.062075>
- 876
- 877 Wilson, P., Wood, C., Walsh, P., Bergman, A., Bergman, H., Laurent, P., & White, B.
878 (2004). Discordance between Genetic Structure and Morphological, Ecological, and
879 Physiological Adaptation in Lake Magadi Tilapia. *Physiological and Biochemical*
880 *Zoology*, 77 (4), 537–555. <https://doi.org/10.1086/422054>
- 881 Wood, C. M., Brix, K. V., De Boeck, G., Bergman, H. L., Bianchini, A., Bianchini, L. F.,
882 ... Ojoo, R. O. (2016). Mammalian metabolic rates in the hottest fish on earth.
883 *Scientific Reports*, srep26990. <https://doi.org/10.1038/srep26990>

- 884 Wood, C. M., & Marshall, W. S. (1994). Ion Balance, Acid-Base Regulation, and
885 Chloride Cell Function in the Common Killifish, *Fundulus heteroclitus*: A
886 Euryhaline Estuarine Teleost. *Estuaries*, *17* (1), 34. <https://doi.org/10.2307/1352333>
887 Zaccara, S., Crosa, G., Vanetti, I., Binelli, G., Harper, D. M., Mavuti, K. M., ... Britton,
888 J. R. (2014). Genetic and morphological analyses indicate high population mixing
889 in the endangered cichlid *Alcolapia* flock of East Africa. *Conservation Genetics*, *15*
890 (2), 429–440. <https://doi.org/10.1007/s10592-013-0551-2>
891 Zanden, M. J. Vander, & Rasmussen, J. B. (1999). Primary consumer $\delta^{13}\text{C}$ and $\delta^{15}\text{N}$
892 and the trophic position of aquatic consumers. *Ecology*, *80* (4), 1395–1404.
893 [https://doi.org/10.1890/0012-9658\(1999\)080\[1395:PCCANA\]2.0.CO;2](https://doi.org/10.1890/0012-9658(1999)080[1395:PCCANA]2.0.CO;2)
894 Zanden, M. J. Vander, & Rasmussen, J. B. (2001). Variation in $\delta^{15}\text{N}$ and $\delta^{13}\text{C}$ trophic
895 fractionation: Implications for aquatic food web studies. *Limnology and*
896 *Oceanography*, *46* (8), 2061–2066. <https://doi.org/10.4319/lo.2001.46.8.2061>
897
898

899 **Acknowledgments**

900 This study was supported by the King Abdullah University of Science and Technology
901 (KAUST). We are very grateful to the KAUST Coastal and Marine Resources Core Lab
902 and KAUST Government Affairs for their support in finding desert ponds, obtaining
903 permits and aiding in the field. We thank the KAUST Integrative Systems Biology
904 Laboratory and the KAUST Biosciences Core Laboratory for support and assistance.

905

906 **Author contributions:** C.S. designed and managed the field collection. C.S, L.C.B &
907 J.N. performed the sample collection. L.C.B. and J.N. with the supervision of C.S.
908 prepared the samples for DNA sequencing and tissue isotope measurements. M.L.B.
909 provided reagents. J.N. performed chemical water analyses and L.C.B. analyzed the
910 tissue isotope data. S.D.P., Y.A.L. and M.F.M. created hydrological mapping and
911 analyzed water isotopes. C.S. analyzed the sequencing data, performed population
912 genetic analyses with help from J.S. and integrated all datasets. C.S. & T.R. wrote the
913 paper; all authors provided input to and approved the final version of the manuscript.

914

915 **Additional information:**

916 Raw sequencing data have been deposited on NCBI under BioProject ID PRJNA311159.
917 Final SNP vcf file is available as Supplementary Material. Correspondence and requests
918 for materials should be addressed to T.R. or C.S.

919

920 **Competing interests**

921 The authors declare no competing interests.

922 Figure legends

923 Figure 1: Locations of all sampling sites over a 1,100 km stretch of the Saudi Arabian
924 coastline. Grey circles represent desert ponds without the presence of *Aphanius dispar*.
925 Sites with pupfish are colored (n=11) and classified as desert ponds (DP) or seawater
926 lagoons (SW). The top two pictures show a male and female *A. dispar*, respectively. The
927 center picture is an example of a desert pond (DP2), below which is the Al Lith hotspring
928 (DP3). The bottom picture shows an example of a seawater site (SW4). The map was
929 created using ArcGIS 10.5 (www.arcgis.com).

930

931 Figure 2: Hydrological modeling. Latitudinal 2D overview of Saudi Arabian coastline
932 with *Aphanius dispar* collection sites indicated with fish icons (left) and 3D close-ups on
933 three regions with predicted hydrological flow. Maps were produced with Google Earth
934 imagery (Google Earth 7.1.2.2041; December 31, 2016) and ArcGIS 10.5 software
935 (www.arcgis.com).

936

937 Figure 3: Heatmap of F_{ST} values of pairwise population comparisons based on 5,955
938 SNPs. Location abbreviations as in Table 1 (DP=desert pond, SW=seawater).

939

940 Figure 4: *Aphanius dispar* population structure with a) $K=4$ and b) $K=8$. Each individual
941 in the different sites (y-Axis) are plotted with colours representing the probability of each
942 individual to be assigned to a certain cluster.

943

944 Figure 5: Scatterplot of principal component analysis evaluating the genetic structure
945 between all analyzed *Aphanius dispar* individuals based on 5,955 loci. Eigenvalues
946 represent the amount of genetic diversity shown by each principal component. a) PCA of
947 principal components 1 and 2. b) PCA of principal components 1 and 3.

948

949 Figure 6: Ratio of stable isotopes of carbon and nitrogen in muscle tissue of *Aphanius*
950 *dispar*, including fish from brackish water ponds and saltwater in the Red Sea. Error bars
951 represent the standard error per location

952

953 Table 1: Sampling locations, characteristics and selected water parameters (for full water
 954 measurements refer to Supplementary Table 1) measured by CTD or Aquakem. A dash
 955 indicates that no reliable measurement was obtained.

Site	Type	Temperature (°C)	Conductivity (µS/cm)	Salinity (ppt)	O2 (ppm)	pH	Chlorides (ppm)	Silica (ppb)	pupfish present
SW5	Sea	21.77	58,340.47	41.93	2.87	8.71	27.10	306.02	yes
SW4	Sea	27.90	66,952.99	42.75	3.39	9.01	29.59	314.61	yes
SW3	Sea	22.82	58,685.99	41.19	4.40	9.10	2.15	104.57	yes
SW2	Sea	24.80	64,966.91	44.20	3.43	8.37	36,677.27	517.96	yes
SW1	Sea	20.90	59,185.03	43.49	3.93	8.37	36.06	31.97	yes
DP6	Pond	31.42	1,663.76	0.74	7.75	9.41	282.41	34,511.49	yes
DP5	Pond	30.93	1,760.39	0.79	8.32	9.39	294.11	59,944.24	yes
DP4	Pond	26.44	2,004.49	0.99	6.14	8.31	278.57	63,358.87	yes
DP3	Hot Spring	38.42	1,916.49	0.75	5.16	8.20	361.21	80,469.67	yes
DP2	Pond	31.58	3,190.00	1.45	4.35	8.31	734.37	38,017.18	yes
DP1	Pond	29.93	1,720.00	0.78	4.35	8.50	469.77	33,586.98	yes
28	Sea	27.65	64,108.41	40.93	3.32	8.46	-	-	no
27	Sea	21.77	65,110.01	47.50	3.81	8.21	-	-	no
26	Sea	18.18	51,228.77	39.44	4.56	8.40	-	-	no
25	Sea	22.60	57,621.28	40.54	3.61	8.48	-	-	no
24	Sea	12.08	46,285.24	41.12	4.11	8.29	-	-	no
23	Sea	21.74	63,528.52	46.35	3.86	8.24	-	-	no
15	Pond	21.28	5,825.19	0.31	6.00	8.60	76.24	20,016.72	no
14	Pond	21.15	8,023.78	0.43	3.10	7.71	115.34	38,414.86	no
13	Pond	-	-	-	-	-	103.07	5,016.26	no
11	Pond	28.91	898.74	0.41	6.33	8.04	86.54	38,664.80	no
9	Pond	33.54	1,025.76	0.43	6.26	9.15	127.94	52,096.62	no
7	Pond	30.21	1,257.23	0.56	4.49	8.05	196.26	76,975.60	no
6	Pond	28.31	1,164.95	0.54	4.69	8.34	128.02	46,885.01	no
5	Pond	30.25	879.72	0.39	4.26	8.11	135.60	25,711.03	no
4	Pond	-	-	-	-	-	29.70	10,464.11	no
3	Pond	21.60	1,019.11	0.54	5.32	8.25	166.66	45,331.00	no

956

957

958 Table 2: Genetic metrics for all 11 pupfish locations for 5,955 SNP loci per sampling site.

959 N = number of individuals, Private a = number of private alleles, Na = average number of

960 alleles, Ho = observed heterozygosity, He = expected heterozygosity, F_{IS} = inbreeding

961 coefficient, Ne = effective population size, 95% CI = 95% confidence intervals for Ne,

962 mean r = average of pairwise kinship coefficient.

Location	N	Private a	Na	Ho	He	F_{IS}	Ne	95% CI	Mean r
DP1	29	15	1.74	0.21	0.23	0.07	1222	983-1614	0.22
DP2	29	8	1.78	0.24	0.25	0.05	1851	1256-3511	0.12
DP3	28	6	1.57	0.17	0.19	0.07	464	421-515	0.12
DP4	27	27	1.31	0.08	0.08	-0.02	51	49-52	0.20
DP5	28	4	1.53	0.16	0.17	0.06	1497	1084-2416	0.25
DP6	29	9	1.50	0.15	0.16	0.09	1713	1236-2782	0.13
SW1	28	7	1.80	0.24	0.27	0.08	1149	882-1646	0.27
SW2	29	13	1.80	0.23	0.26	0.09	5910	2229-inf	0.06
SW3	29	0	1.66	0.19	0.20	0.06	1702	1199-2925	0.15
SW4	30	0	1.77	0.20	0.22	0.10	1645	1284-2286	0.19
SW5	28	0	1.70	0.18	0.20	0.12	3917	2175-19493	0.42

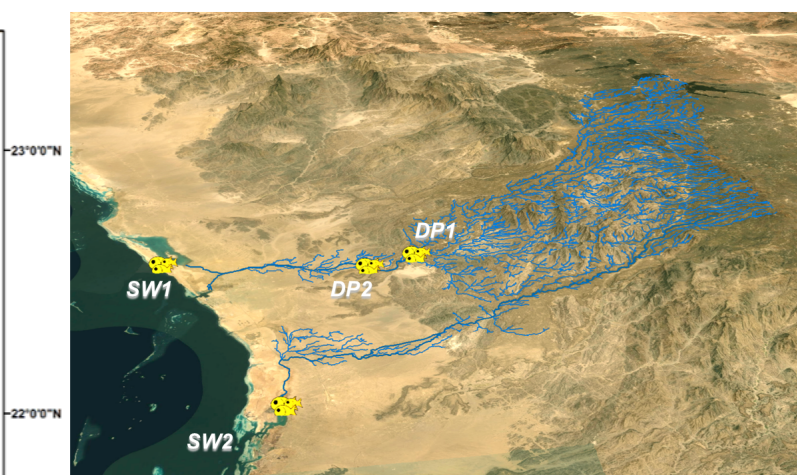
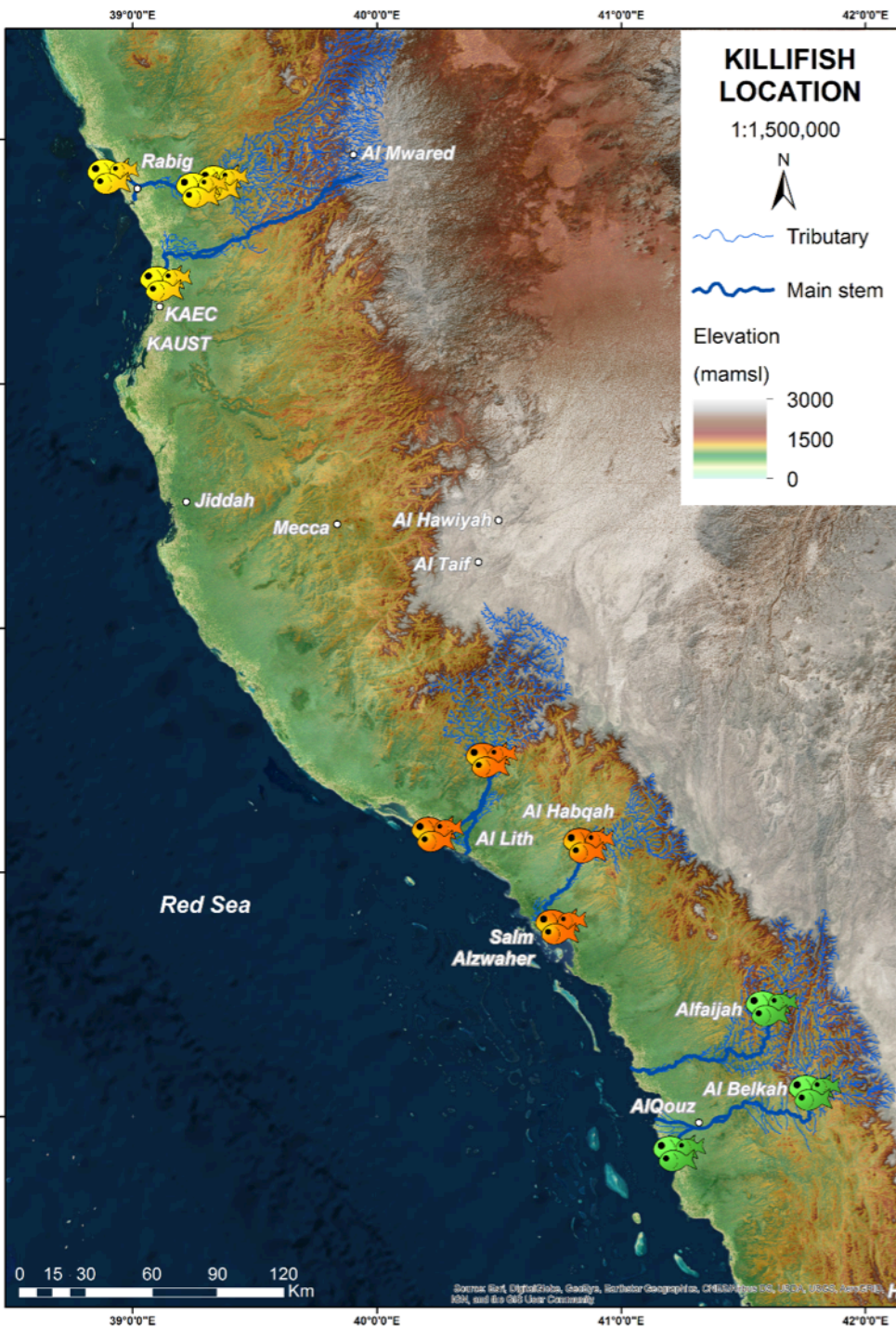
963

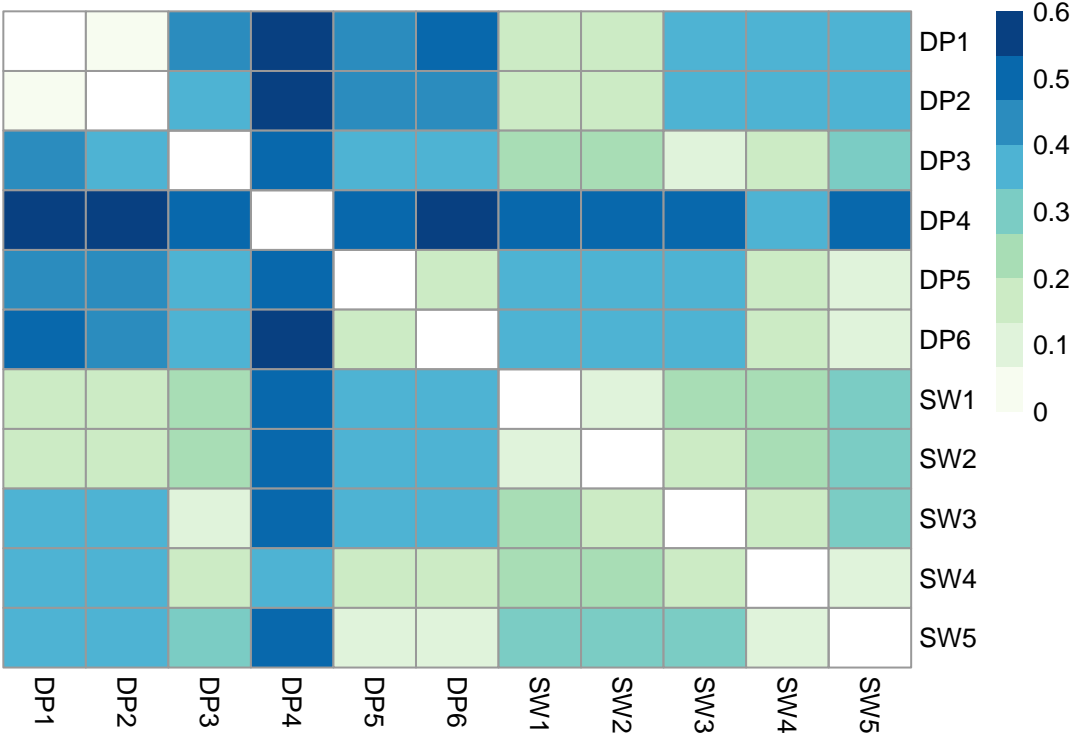
964

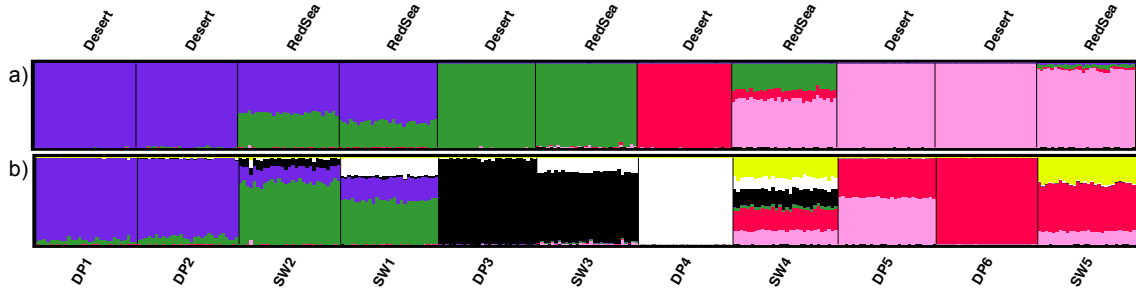
965 Table 3: Putative outlier loci between desert pond and red sea locations. Several pairwise
 966 comparisons were performed, and the compared locations are indicated under “Locations
 967 included”. Sequences were blasted again NCBI and only successful blast hits are listed.

Locations included: DP	Locations included: SW	SNP loci included	Number of outliers	SNP name	NCBI description	Species of best blast hit	gene name	e-value	coverage	NCBI accession	
DP all	SW all	4507	5	19937_75							
				35939_106	perforin-1-like	<i>Salmo salar</i>	perf	2.00E-05	86%	XM_014185448.1	
				76967_58							
				90197_26	integrin alpha-6-like	<i>Poecilia formosa</i> <i>Nothobranchius furzeri</i>	itga6	3.00E-10	79%	XM_016678011.1	
				112486_90	AFG3-like protein 1	<i>furzeri</i>	afg3	8.00E-30	95%	XM_015952175.1	
DP1&DP2	SW1&SW2	2449	1	90197_30	integrin alpha-6-like unchar. protein	<i>Poecilia formosa</i>	itga6	3.00E-10	79%	XM_016678011.1	
DP1&DP2	SW1	2586	1	126619_29	K02A2.6-like	<i>Oreochromis niloticus</i>		4.00E-08	75%	XM_019364105.1	
DP1&DP2	SW2	2890	6	26511_91							
				33001_35							
				76967_58							
				90197_30	integrin alpha-6-like	<i>Poecilia formosa</i>	itga6	3.00E-10	79%	XM_016678011.1	
				107780_39	potassium voltage-gated channel subfamily H member 2-like	<i>Poecilia mexicana</i>	kcnh2	0.003	70%	XM_014994260.1	
DP3	SW3	3704	1	116615_106	AFG3-like protein 1			8.00E-30	95%	XM_015952175.1	
DP4	SW4	2631	1	112486_90		<i>Nothobranchius furzeri</i>					
DP5&DP6	SW5	3963	10	19073_13	immunoglobulin light chain genomic sequence	<i>Takifugu rubripes</i>		0.003	84%	KU365392.1	
				20996_81							
				39387_14							
				62495_79							
				63109_75	v-rel avian reticuloendotheliosis viral oncogene homolog	<i>Nothobranchius furzeri</i>	rel	1.00E-21	82%	XM_015944097.1	
				67796_71							
				68351_79	piezo type mechanosensitive ion channel component 1 zinc finger MIZ domain-containing	<i>Nothobranchius furzeri</i>	piezo1	2.00E-05	73%	XM_015945536.1	
				80013_20	protein 1-like uncharacterized	<i>Astyanax mexicanus</i>	zbtb17	3.00E-22	89%	XM_007235440.2	
83760_40	LOC103909955	<i>Danio rerio</i>		5.00E-07	81%	XM_017354508.1					
				89871_81							
DP4	SW all	4761	1	19939_80							

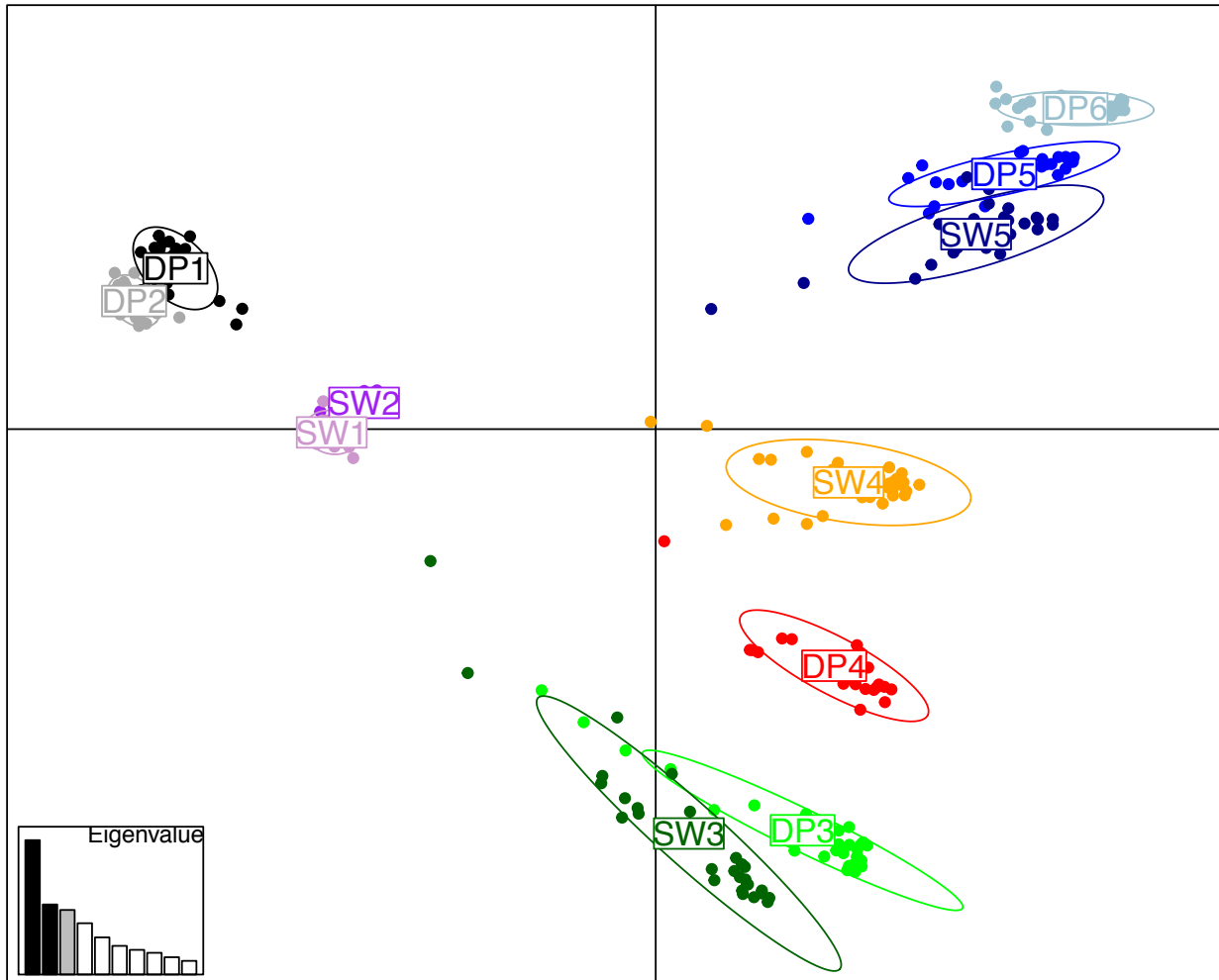
968



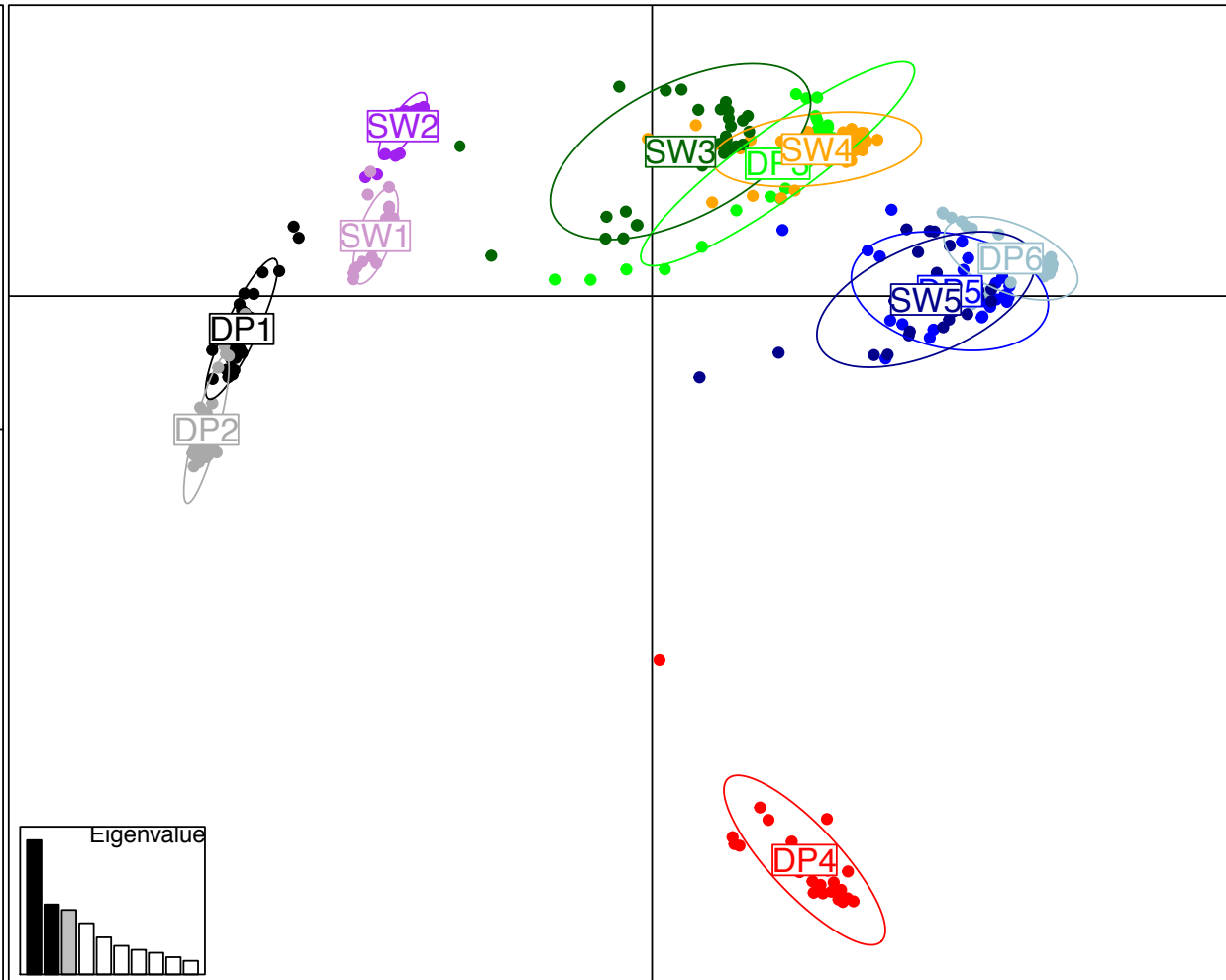


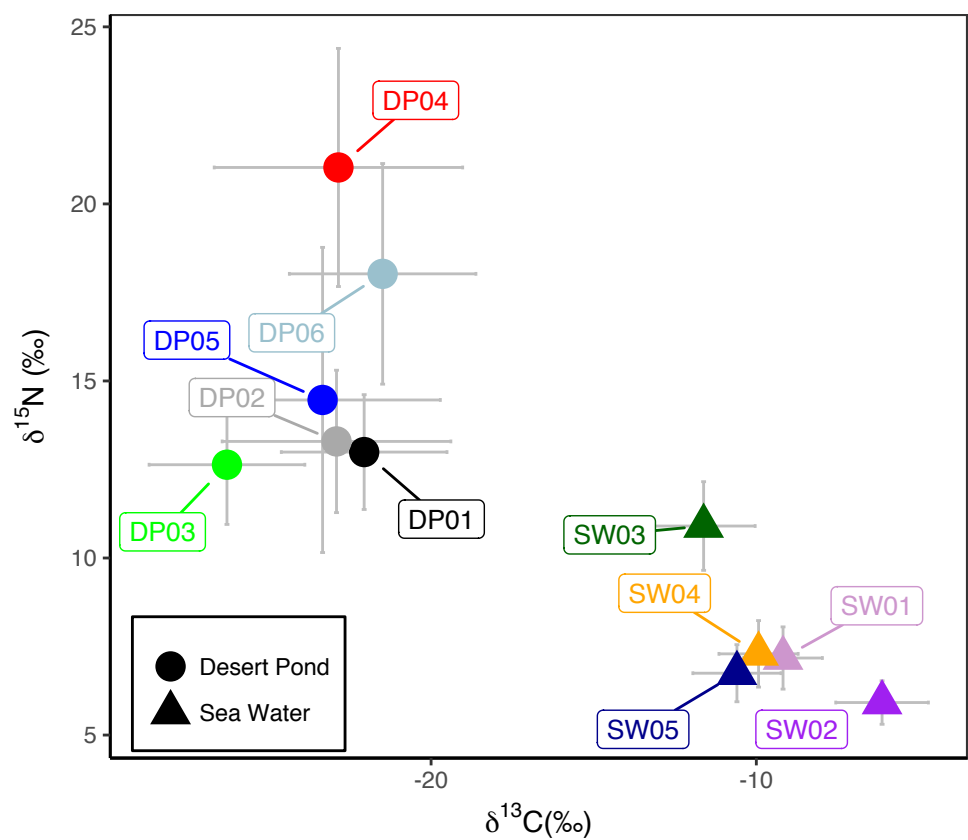


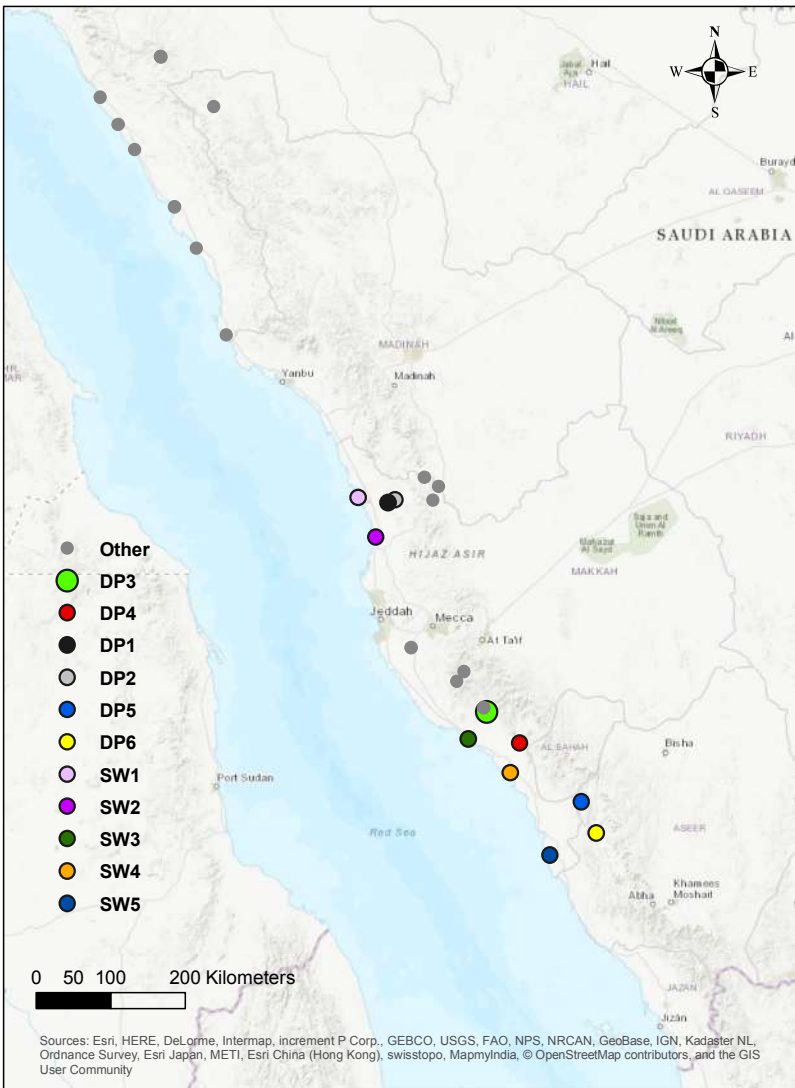
a)



b)







Sources: Esri, HERE, DeLorme, Intermap, increment P Corp., GEBCO, USGS, FAO, NPS, NRCAN, GeoBase, IGN, Kadaster NL, Ordnance Survey, Esri Japan, METI, Esri China (Hong Kong), swisstopo, MapmyIndia, © OpenStreetMap contributors, and the GIS User Community